2010

Incorporation of Europium (III) coordination compounds into silica microspheres

Johnathan Nathanael Brantly
Western Kentucky University

INCORPORATION OF EUROPIUM(III) COORDINATION COMPOUNDS INTO SILICA MICROSPHERES

A Capstone Experience/Thesis Project

Presented in Partial Fulfillment of the Requirements for

the Degree Bachelor of Science with

Honors College Graduate Distinction at Western Kentucky University

By

Johnathan Nathanael Brantley

*****

Western Kentucky University
2010

CE/T Committee:

Dr. Les Pesterfield, Advisor

Dr. Stuart Burris

Dr. Michael Smith

Approved By

Advisor
Department of Chemistry

ABSTRACT

The unique optical properties of silica microspheres and lanthanoid elements present the opportunity to adapt silica microspheres containing rare earth elements for novel optical applications. The research demonstrates the first example of incorporating insoluble lanthanoid coordination compounds into silica microspheres. The work explored the controlled synthesis of silica microspheres and the reaction conditions under which lanthanoid complexes can be incorporated into the microspheres. The environment of the coordinated lanthanoid ions before and after incorporation into silica microspheres was probed using spectroflurophotometry. The surface morphology of silica microspheres was characterized using atomic force microscopy (AFM) and scanning electron microscopy (SEM). The work explored novel syntheses of lanthanoid monoporphyrinates. The work also explored the incorporation of porphyrin macrocycles into silica microspheres.

Keywords: Lanthanoid, Silicate, Microspheres, Incorporation, Luminescence

Dedicated to Doc, Al, Niki, CJ, Erica, and my family

ACKNOWLEDGEMENTS

This work would not have been possible without support from the Department of Chemistry, Ogden College in the form of the Ogden Research Scholarship, and the Western Kentucky University Honors Center in the form of an Honors Development Grant. Special gratitude is extended to Dr. John Andersland, Dr. Stuart Burris, Dr. Kevin Williams, Mr. Michael Starling, and Mr. Kevin Kerian.

VITA

February 2, 1988……Born – Marion, Kentucky

2006……Crittenden County High School, Marion, Kentucky

2006……Chemical Stockroom Assistant, Western Kentucky University

2009……WKU-Oxford Summer Research Fellowship, University of Oxford

FIELDS OF STUDY

Major Field: Chemistry (ACS Certified)

Minor Field: Mathematics

TABLE OF CONTENTS

LIST OF SCHEMES, TABLES, FIGURES, AND IMAGES

Image

CHAPTER 1

INTRODUCTION

The unique optical properties of silica microspheres and lanthanoid elements are well known. Silica microspheres and micro silicates containing luminescent dyes or quantum dots have been used in optical encoding[1-4], bioanalysis[5-11], and quantum-optical studies[12-14]. The optical properties of silica microspheres and sol-gels containing lanthanoid ions, however, have generated recent interest. Microspheres and sol-gels containing lanthanoid ions have found applications as scintillators[15-17], optical fiber amplifiers[18,19], lasers[20,21], and biosensors.[22] The characteristic narrow bandwidths associated with the photonic emission from excited lanthanoid ions make these luminescent entities particularly appealing for optical applications. The shielding of the lanthanoid 4f subshell by the $6s^2$ and $5p^6$ subshells results in parity-forbidden 4f-4f absorptions that have low molar absorptivity coefficients and narrow-line emission[23]. Lanthanoid luminescence essentially depends upon the energy gap between the lowest energy emissive state of the metal ion and the highest sublevel of the ground state, with larger gaps favoring luminescence rather than non-radiative relaxation processes (such as vibration of bound ligands).[23] The europium(III) cation, which has an energy gap of 12,300 cm^{-1} for the $^5D_0 \rightarrow {}^7F_6$ transition, has one of the largest energy gaps of all lanthanoid trivalent cations.[23] Due to the nature of the 4f-4f transition responsible for lanthanoid

luminescence, direct excitation of trivalent lanthanoid ions rarely results in substantial photonic emission.[23] Indirect excitation, or sensitization, of the metal ion through ligands must therefore be used. This sensitization process is initiated when photons impinge upon chromophores within the coordination sphere of the metal ion. The resulting energy that is absorbed by the ligands is transferred to the metal center, excites electrons to an emissive state, and ultimately results in photonic emission from the metal.[23] The emission of lanthanoid ions, then, can be significantly enhanced if the ion is coordinated to appropriate ligands.[24-26] As an example, porphyrin ring systems are enticing ligands because these highly conjugated macrocycles have the potential to serve as "antennas" capable of harvesting photons. The energy harvested from these photons can be readily transferred to the coordinated metal center, a fact that is demonstrated by the luminescence of lanthanoid porphyrinates.[27] While certain ligands sensitize rare earth ions, other ligands are capable of quenching lanthanoid luminescence. Ligands containing hydroxyl functionalities (i.e. water) are particularly efficient quenchers of lanthanoid luminescence because these ligands allow the transfer of vibrational energy from the excited metal center.[23] The displacement of water ligands from the coordination sphere of lanthanoid ions, then, would enhance the emissive properties of the metal center. A potential method for displacing, or at least limiting, water ligands coordinated to a lanthanoid ion could involve chelation of the metal followed by incorporation of the resulting complex into a silica microsphere. As such, the ability to incorporate highly luminescent, insoluble lanthanoid complexes into silica microspheres presents the opportunity to develop a new class of novel optical sensors.

Incorporation of lanthanoid ions into silica microspheres, however, presents synthetic obstacles. Silica microspheres are traditionally prepared using a modification of the Stöber process[28], a hydrolysis reaction with concomitant polymerization that is catalyzed by basic moieties, that involves the condensation of tetraethylorthosilicate (TEOS) in ethanol:water mixtures. Lanthanoid ions form insoluble salts in basic media, however, and this necessitates the use of an acid-catalyzed preparation (see Scheme 1).[29]

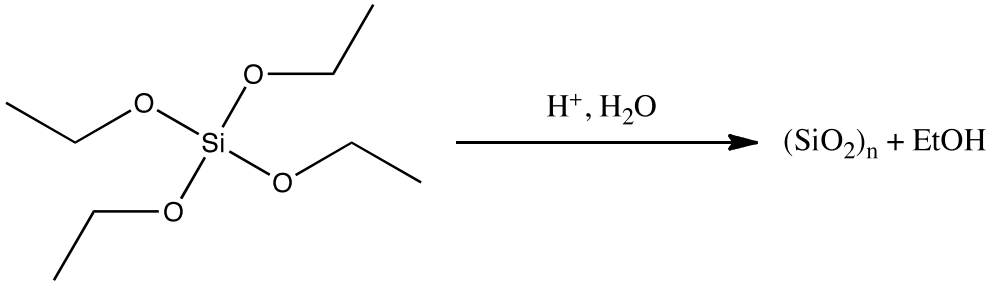

Scheme 1: Acid-Catalyzed Hydrolysis of TEOS

In addition, while the incorporation of lanthanoid ions into silica microspheres and sol-gels has been studied extensively, the incorporation of insoluble lanthanoid coordination compounds into silica microspheres has not been explored.

This work explores the controlled synthesis of silica microspheres from an acid-catalyzed hydrolysis reaction. Silicates prepared from acid-catalyzed reaction schemes are notoriously polydisperse in comparison to the particles generated under basic conditions. The intimate relationship between particle size and optical properties of silica microspheres lends considerable importance to the controlled synthesis of monodisperse particles.[30] In an effort to elucidate potential surface interactions that influence particle size distribution, the surface morphology of the microspheres was characterized using atomic force microscopy (AFM). The incorporation of insoluble europium(III) coordination compounds into silica microspheres, and the resulting optical properties of

the doped microspheres, has been explored. Specifically, the work has explored the incorporation of silver (ethlenediaminetetraacetato)europate(III) and potassium tetrakis(2,4-pentanediono)europate(III) into silica microspheres. The coordination spheres of the doped europium(III) ions were explored using spectrofluorophotometry. The synthesis of europium(III) monoporphyrinates was also explored. The work investigated novel reaction conditions with the desire to develop a more environmentally orthogonal synthesis of these compounds. Due to time constraints, this aspiration was never fully realized. The work explored the incorporation of 5,10,15,20-Tetra(4-Pyridyl)-21H,23H porphine into silica microspheres in an effort to demonstrate the feasibility of doping micro silicates with lanthanoid porphyrinates.

CHAPTER 2

EXPERIMENTAL

Synthesis of Silica Microspheres

Silica Microspheres were prepared through the acid-catalyzed hydrolysis of tetraethoxyorthosilicate (TEOS). TEOS (4.5 mL, 0.020 mol) was added to a glass beaker in an ice bath. Glacial acetic acid (9.0 mL, 0.16 mol), ethyl alcohol (95%, 1.2 mL, 0.020 mol), and deionized water (0.40 mL, 0.020 mol) were combined in a separate glass beaker. The acidified ethanol solution (5.5 mL) was cooled in an ice bath and then added drop-wise to the TEOS with stirring. Addition of the acidified ethanol solution took approximately 3 minutes, and the rate of mixing was set at approximately 300 rpm. The reaction mixture was stirred for approximately 15 minutes upon complete addition of the ethanol solution. The reaction mixture was then cooled in a refrigerator for approximately 3 hours, after which time the polymerization reaction was quenched through decanting of the mother liquor. The white microspheres were washed with cold ethyl alcohol (95%, 3 X 5 mL) and cold acetone (3 X 5 mL). The glass beaker was covered with parafilm, and the microspheres were allowed to dry for a period of 24 hours. The dried silica microspheres were collected and characterized using scanning electron microscopy (SEM) and atomic force microscopy (AFM).

Synthesis of Ag[Eu(EDTA)] Coordination Compound

Silver (ethlenediaminetetraacetato)europate(III) was synthesized according to the procedure developed by Pesterfield.[31] Europium(III) oxide (0.20 g, 0.57 mmol) and ethylenediaminetetraacetic acid (EDTA, 0.33 g, 1.1 mmol) were added to deionized water (20.0 mL). Dissolution of the reagents was achieved with sufficient heating (50° C) and stirring. The mother liquor was allowed to cool slowly to room temperature, and silver nitrate (0.19 g, 1.1 mmol) was added to the reaction mixture. Sodium hydroxide (0.1M solution in deionized water) was added drop-wise until a white precipitate formed. The mother liquor was decanted, and the precipitate was washed with deionized water (3 X 10 mL). The coordination compound was suspended in deionized water and protected from light sources.

Synthesis of K[Eu(acac)$_4$]

Potassium tetrakis(2,4-pentanediono)europate(III) was synthesized according to a modification of the literature preparation of sodium tetrakis(1-phenyl-1,3-butanediono)europate (III) developed by Murray.[32] Acetone (50.0 mL), 2,4-pentanedione (1.03 mL, 0.01 mol), and potassium hydroxide (0.56 g, 0.01 mol) were added to a Florence flask. The reaction mixture was heated to reflux for approximately 30 minutes. A solution of europium(III) chloride was prepared through the dissolution of europium(III) oxide (1.00 g, 2.84 mmol) in concentrated hydrochloric acid (1.42 mL, 17.04 mmol) and deionized water (8.58 mL). An aliquot of the freshly prepared

europium(III) chloride solution (3.52 mL, 1.0 mmol) was diluted with deionized water (10.00 mL). The diluted europium(III) chloride solution was added drop-wise to the refluxed acetone mixture. The resulting reaction mixture was then refluxed for one hour. The mixture was then cooled in a refrigerator for 24 hours. The pale-yellow microcrystals that precipitated from solution were collected via filtration and dried *in vacuo* for approximately 10 minutes. The microcrystals were annealed for 24 hours at a temperature of 110° C. The annealed microcrystals were allowed to cool slowly to room temperature and stored in a dessicator.

Synthesis of Europium (III) Monoporphyrinate Complexes

The synthesis of a monoporphyrinate complex with europium (III) using 5,10,15,20-Tetra(4-pyridyl)-21H, 23H porphine was attempted. Traditional syntheses of monoporphyrinate and "double-decker" (both heteroleptic and homoleptic) complexes with europium(III) require toxic solvents and reagents. Anhydrous conditions in an inert atmosphere are also typically required.[27,33,34] There is a literature example of the synthesis of monoporphyrinate complexes with europium(III) under atmospheric conditions, however. The research attempted numerous syntheses with environmentally orthogonal solvents under atmospheric conditions that were modifications of the literature procedure developed by Wong.[35] The target product was not isolated under the experimental conditions that were explored. Table 1 presents the synthetic parameters

explored in the pursuit of more environmentally orthogonal syntheses of monoporphyrinate lanthanoid complexes.

Table 1: Attempted Syntheses of Monoporphyrinate

Por* (g)	$EuCl_3$ (g)	$Eu(NO_3)_3$ (g)	$K[Eu(AcAc)_4$ (g)	HCl (μL)	Solvent	Temp (C)	Rxn Time (h)	Pdt. Isolation
0.20	0.05	0.00	0.00	29.35	Water	25	96	Precipitation With NaOH
0.11	0.00	0.04	0.00	58.70	Water	100	24	Precipitation With NaOH
0.02	0.00	0.00	0.01	0.00	Pentanol	138	96	Column
0.21	0.00	0.00	0.10	0.00	TCB**	214	5	Column

* - 5,10,15,20-Tetra(4-Pyridyl)-21H,23H porphine

** - 1,2,4-Trichlorobenzene

Incorporation of Ag[Eu(EDTA)] Coordination Complex Into Silica Microspheres

TEOS (4.5 mL, 0.02 mol) was added to a glass beaker in an ice bath. Glacial acetic acid (9.0 mL, 0.16 mol), ethyl alcohol (95%, 1.2 mL, 0.02 mol), silver (ethylenediaminetetraacetato)europate(III) (2 drops of suspension, *vide supra*), and deionized water (0.40 mL, 0.02 mol) were combined in a separate glass beaker. The acidified ethanol solution (5.5 mL) was cooled in an ice bath and then added drop-wise to

the TEOS with stirring. Addition of the acidified ethanol solution took approximately 3 minutes, and the rate of mixing was set at approximately 300 rpm. The reaction mixture was stirred for approximately 15 minutes upon complete addition of the ethanol solution. The reaction mixture was cooled in a refrigerator for approximately 3 hours, after which time the polymerization reaction was quenched through decanting of the mother liquor. The white microspheres were washed with cold ethyl alcohol (95%, 3 X 5 mL) and cold acetone (3 X 5 mL). The glass beaker was covered with parafilm, and the micro silicates were allowed to dry for a period of 24 hours. The dried microspheres were collected and characterized using SEM and spectrofluorophotometry.

Incorporation of $K[Eu(acac)_4]$ Coordination Complex Into Micro Silicates

TEOS (4.5 mL, 0.020 mol) was added to a glass beaker in an ice bath. Glacial acetic acid (9.0 mL, 0.16 mol), ethyl alcohol (95%, 1.2 mL, 0.02 mol), potassium tetrakis(2,4-pentanediono) europium(III) (0.01 g, *vide supra*), and deionized water (0.40 mL, 0.02 mol) were combined in a separate glass beaker. The acidified ethanol solution (5.5 mL) was cooled in an ice bath and then added drop-wise to the TEOS with stirring. Addition of the acidified ethanol solution took approximately 3 minutes, and the rate of mixing was set at approximately 300 rpm. The reaction mixture was stirred for approximately 15 minutes upon complete addition of the ethanol solution. The reaction mixture was cooled in a refrigerator for approximately 3 hours, after which time the polymerization reaction was quenched through decanting of the mother liquor. The white microspheres were

washed with cold ethyl alcohol (95%, 3 X 5 mL) and cold acetone (3 X 5 mL). The glass beaker was covered with parafilm, and the microspheres were allowed to dry for a period of 24 hours. The dried microspheres were collected and characterized using SEM and spectrofluorophotometry.

Incorporation of Porphyrin Macrocycle Into Micro Silicates

TEOS (4.5 mL, 0.020 mol) and 5,10,15,20-Tetra(4-pyridyl)-21H, 23H porphine (0.0030 g, 0.010 mmol) were added to a glass beaker in an ice bath. Glacial acetic acid (9.0 mL, 0.16 mol), ethyl alcohol (95%, 1.2 mL, 0.020 mol), and deionized water (0.40 mL, 0.020 mol) were combined in a separate glass beaker. The acidified ethanol solution (5.5 mL) was cooled in an ice bath and then added drop-wise to the TEOS with stirring. Addition of the acidified ethanol solution took approximately 3 minutes, and the rate of mixing was set at approximately 300 rpm. The reaction mixture was stirred for approximately 15 minutes upon complete addition of the ethanol solution. The reaction mixture was cooled in a refrigerator for approximately 3 hours, after which time the polymerization reaction was quenched through decanting of the mother liquor. The dark green microspheres were washed with cold ethyl alcohol (95%, 3 X 5 mL) and cold acetone (3 X 5 mL). The glass beaker was covered with parafilm, and the microspheres were allowed to dry for a period of 24 hours. The dried, orange microspheres were then collected and characterized using SEM and spectrofluorophotometry.

CHAPTER 3

Results

Preparation of the silica microspheres (*vide supra*) resulted in particles with an average diameter of 3.0 μm (σ = 0.6 μm). The reported experimental parameters represent the reaction conditions that were adjusted to limit polydispersity and promote particle uniformity. Electron micrographs and atomic force micrographs of the silicates are presented.

Image 1: Electron Micrograph of Micro Silicates

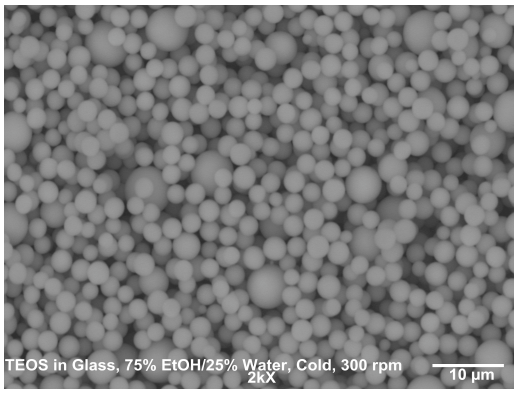

The electron micrographs in Images 1 and 2 demonstrate the relative monodispersity and uniformity of the microspheres prepared according to the reported synthesis.

Image 2: Electron Micrograph of Micro Silicates

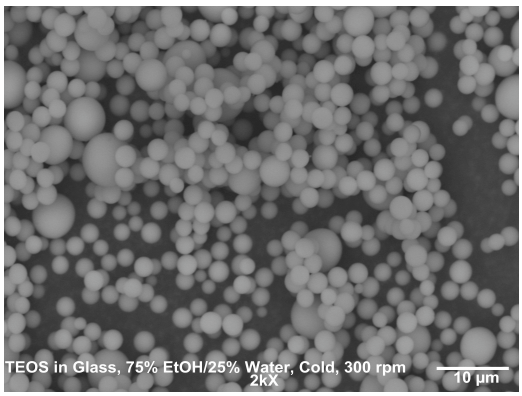

Image 3: Deflection Image of Micro Silicate Surface

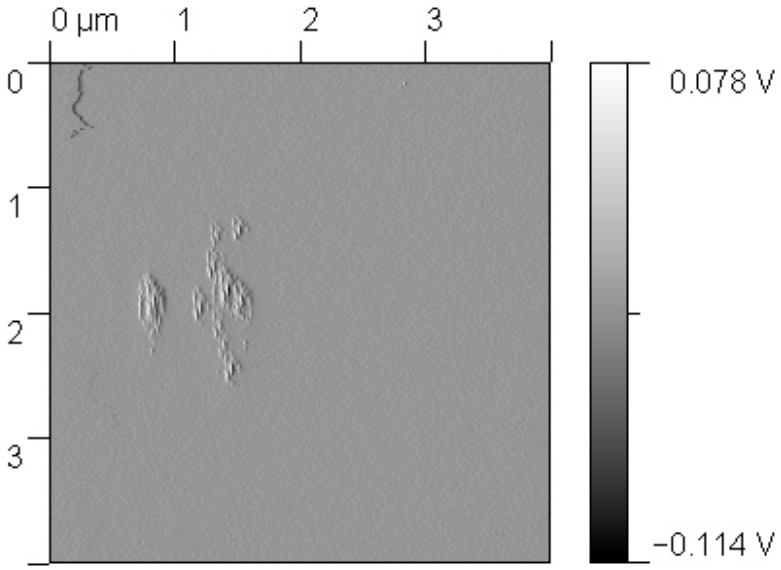

Image 4: Topography Image of Micro Silicate

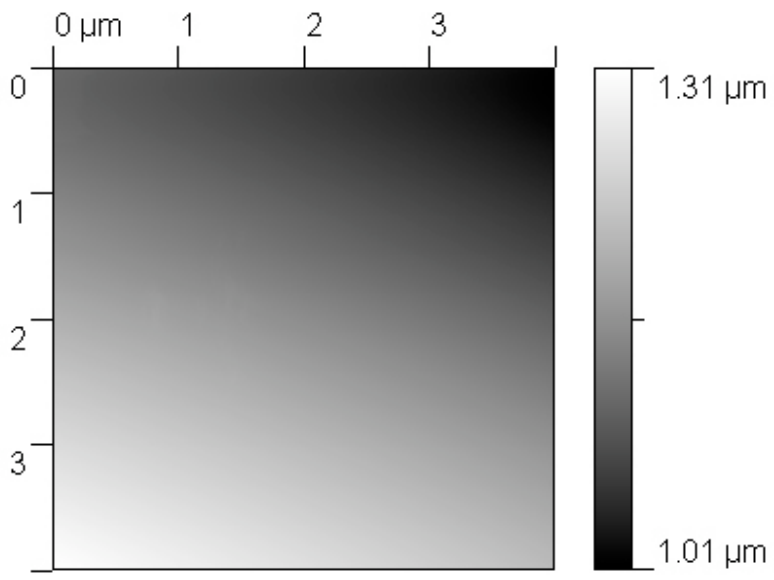

The atomic force micrograph in Image 3 shows the surface morphology of a silica microsphere. The micrograph demonstrates the relative uniformity of the particle surface. While there are some surface features visible, these surface structures are on the nanometer scale; thus, the surface of the particle is relatively smooth and uniform. The micrograph in Image 4 displays the surface topography of a microsphere. The micrograph represents the relative uniformity of the surface of the microsphere.

Several additional preparations of the silica microspheres were attempted; however, the silicates generated under these parameters displayed a higher degree of polydispersity or undesirable characteristics (i.e. twinning and aggregation). Tables 2-4 present these reaction parameters and resulting particle size distributions. Electron micrographs of the samples are also presented in Images 5-24.

Table 2: Additional Preparations of Acidified Solutions

Sample	Ethanol (mL)	Water (mL)	Acetic Acid (mL)
A	0.0	2.2	18.0
B	0.0	2.2	18.0
C	0.0	2.2	18.0
D	0.0	2.2	18.0
E	0.0	2.2	18.0
F	0.0	2.2	18.0
G	0.0	2.2	18.0
H	0.0	2.2	18.0
I	0.0	2.2	18.0
J	0.0	2.2	18.0
K	0.0	2.2	18.0
L	0.0	2.2	18.0
M	0.0	2.2	18.0
N	0.0	2.2	18.0
O	0.0	2.2	18.0
P	0.0	2.2	18.0
Q	0.0	2.2	18.0
R	0.0	2.2	18.0
S	0.4	1.2	9.0
T	0.8	0.8	9.0
U	1.3	0.3	9.0

V	1.4	0.2	9.0
W	1.6	0.0	9.0

Table 3: Additional Synthetic Parameters

Sample	Vessel	Stir Rate (rpm)	Temperature (° C)	Acidic Soln (mL)	TEOS (mL)
A	PP*	300	25	5.5	4.5
B	G**	300	25	5.5	4.5
C	T***	300	25	5.5	4.5
D	PP	400	25	5.5	4.5
E	G	400	25	5.5	4.5
F	T	400	25	5.5	4.5
G	PP	300	40	5.5	4.5
H	G	300	40	5.5	4.5
I	T	300	40	5.5	4.5
J	PP	400	40	5.5	4.5
K	G	400	40	5.5	4.5
L	T	400	40	5.5	4.5
M	PP	300	0	5.5	4.5
N	G	300	0	5.5	4.5
O	T	300	0	5.5	4.5
P	PP	400	0	5.5	4.5
Q	G	400	0	5.5	4.5

R	T	400	0	5.5	4.5
S	G	300	0	5.5	4.5
T	G	300	0	5.5	4.5
U	G	300	0	5.5	4.5
V	G	300	0	5.5	4.5
W	G	300	0	5.5	4.5

* -Glass Beaker
** - Polypropylene Beaker
*** - Teflon Beaker

Table 4: Particle Size Distributions

Sample	Avg. Diameter (μm)	Standard Deviation (μm)
A	4.3	1.5
B	4.9	2.9
C	4.9	1.7
D	4.8	1.7
E	6.5	2.2
F	6.1	1.9
G	6.3	1.7
H	7.2	1.7
I	5.7	2.3
J	6.0	1.8
K	6.5	2.3
L	6.6	1.6
M	4.0	2.2

N	2.8	0.5
O	2.8	1.1
P	3.7	1.7
Q	3.7	1.4
R	3.7	2.3
S	3.9	1.9
T	2.7	0.7
U	No Product Recovered	-
V	No Product Recovered	-
W	No Product Recovered	-

Image 5: Electron Micrograph of Sample A

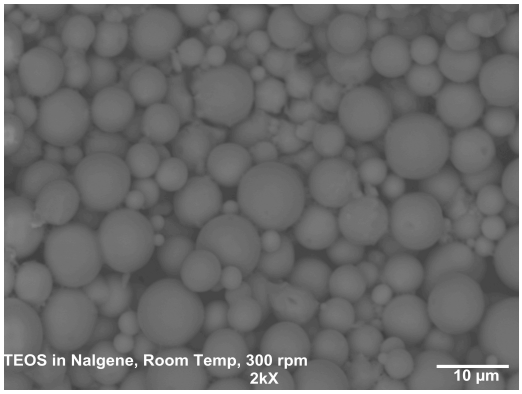

The micrograph in Image 5 demonstrates the relatively polydisperse nature of sample A. In addition, the micrograph displays aggregation of particles and particles with irregular surface morphologies.

Image 6: Electron Micrograph of Sample B

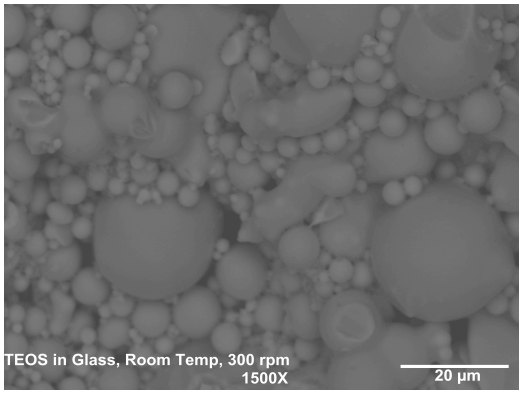

The micrograph in Image 6 demonstrates the relatively polydisperse nature of sample B. In addition, the micrograph displays aggregation of particles and particles with irregular surface morphologies.

Image 7: Electron Micrograph of Sample C

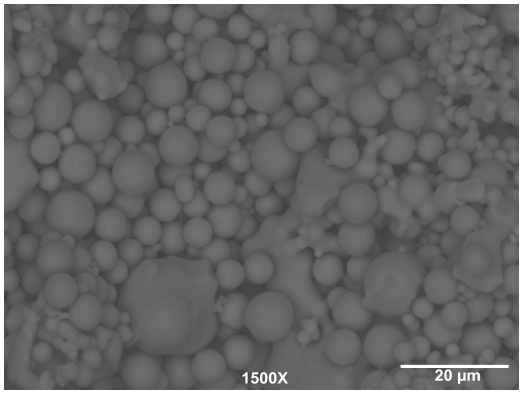

The micrograph in Image 7 demonstrates the relatively polydisperse nature of sample C. In addition, the micrograph displays aggregation of particles and particles with irregular surface morphologies.

Image 8: Electron Micrograph of Sample D

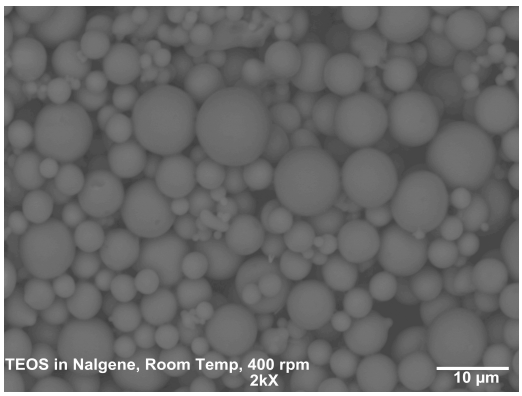

The micrograph in Image 8 demonstrates the relatively polydisperse nature of sample D. In addition, the micrograph displays aggregation of particles and particles with irregular surface morphologies.

Image 9: Electron Micrograph of Sample E

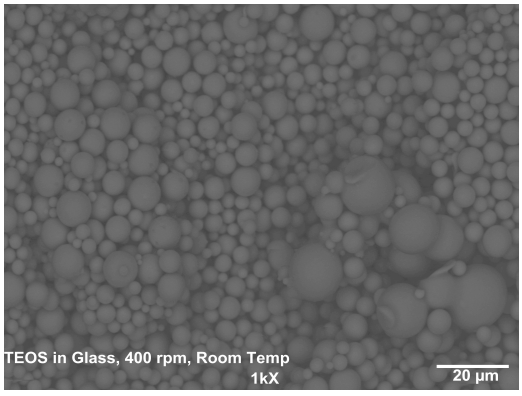

The micrograph in Image 9 demonstrates the relatively polydisperse nature of sample E. In addition, the micrograph displays aggregation of particles and particles with irregular surface morphologies.

Image 10: Electron Micrograph of Sample F

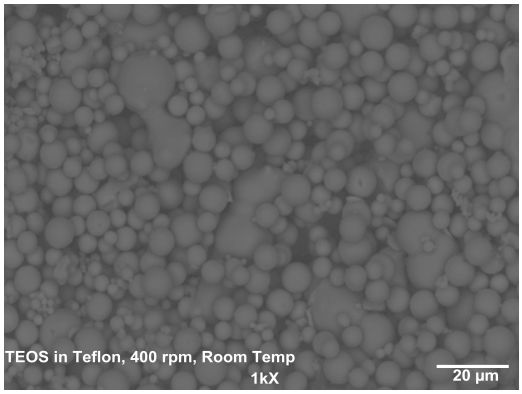

The micrograph in Image 10 demonstrates the relatively polydisperse nature of sample F. In addition, the micrograph displays aggregation of particles and particles with irregular surface morphologies.

Image 11: Electron Micrograph of Sample G

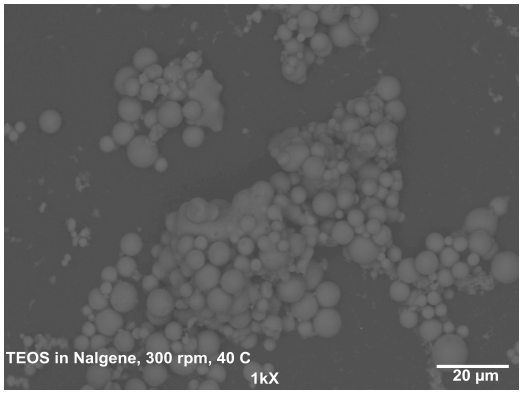

The micrograph in Image 11 demonstrates the relatively polydisperse nature of sample G. In addition, the micrograph displays aggregation of particles and particles with irregular surface morphologies.

Image 12: Electron Micrograph of Sample H

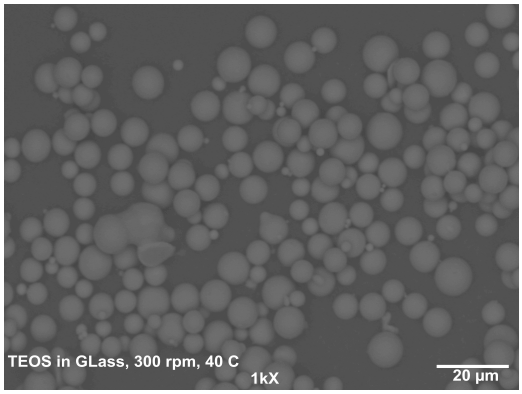

The micrograph in Image 12 demonstrates the relatively polydisperse nature of sample H. In addition, the micrograph displays aggregation of particles and particles with irregular surface morphologies.

Image 13: Electron Micrograph of Sample I

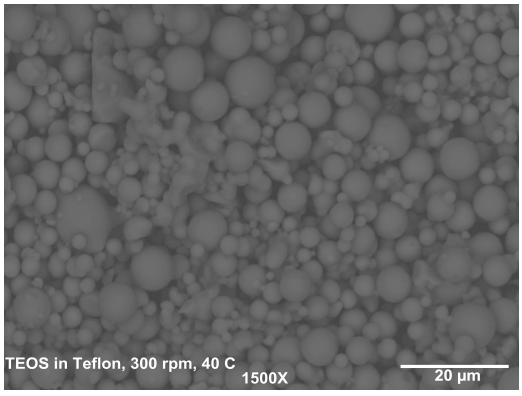

The micrograph in Image 13 demonstrates the relatively polydisperse nature of sample I. In addition, the micrograph displays aggregation of particles and particles with irregular surface morphologies.

Image 14: Electron Micrograph of Sample J

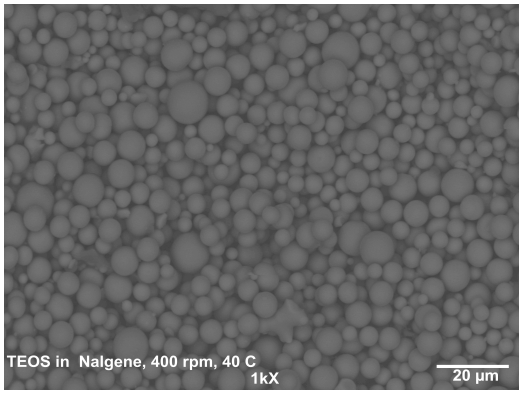

The micrograph in Image 14 demonstrates the relatively polydisperse nature of sample J. In addition, the micrograph displays aggregation of particles and particles with irregular surface morphologies.

Image 15: Electron Micrograph of Sample K

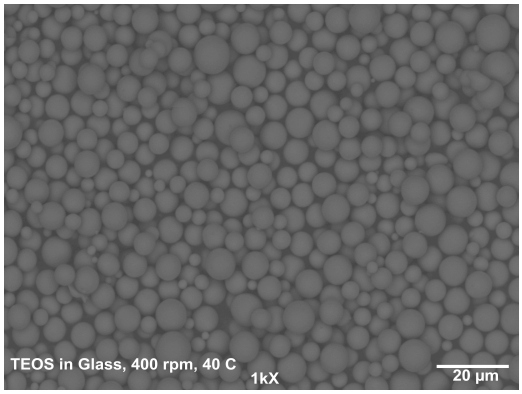

The micrograph in Image 15 demonstrates the relatively polydisperse nature of sample K.

Image 16: Electron Micrograph of Sample L

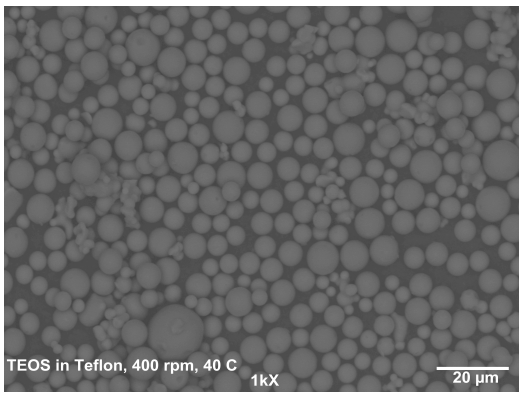

The micrograph in Image 16 demonstrates the relatively polydisperse nature of sample L. In addition, the micrograph displays aggregation of particles and particles with irregular surface morphologies.

Image 17: Electron Micrograph of Sample M

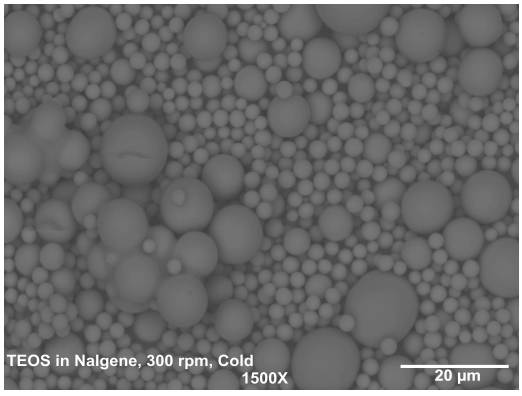

The micrograph in Image 17 demonstrates the relatively polydisperse nature of sample M. In addition, the micrograph displays aggregation of particles and particles with irregular surface morphologies.

Image 18: Electron Micrograph of Sample N

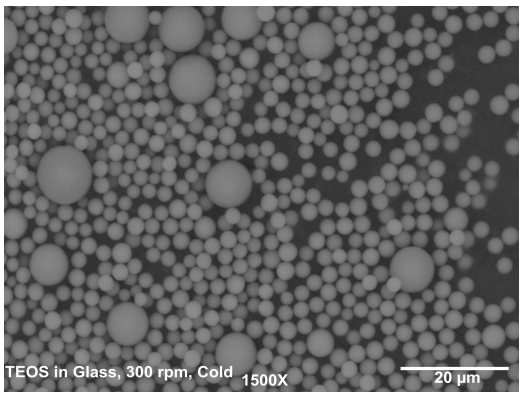

The micrograph in Image 18 demonstrates the relatively polydisperse nature of sample N.

Image 19: Electron Micrograph of Sample O

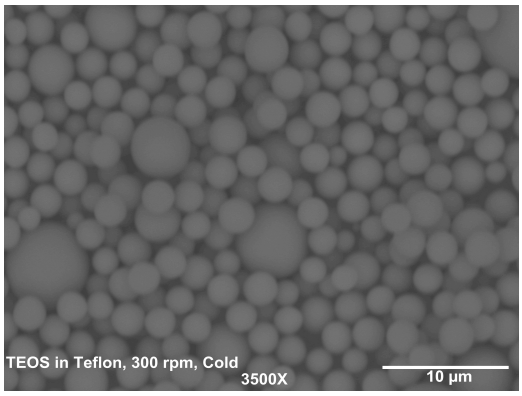

The micrograph in Image 19 demonstrates the relatively polydisperse nature of sample O.

Image 20: Electron Micrograph of Sample P

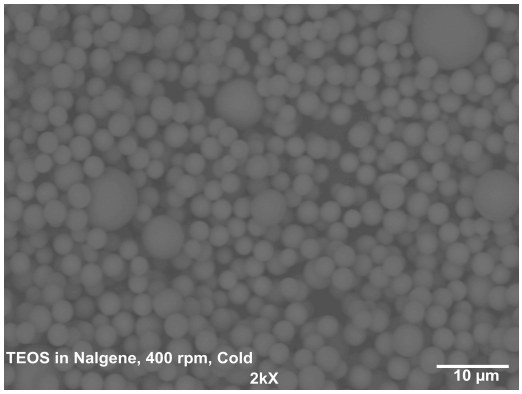

The micrograph in Image 20 demonstrates the relatively polydisperse nature of sample P. In addition, the micrograph displays aggregation of particles and particles with irregular surface morphologies.

Image 21: Electron Micrograph of Sample Q

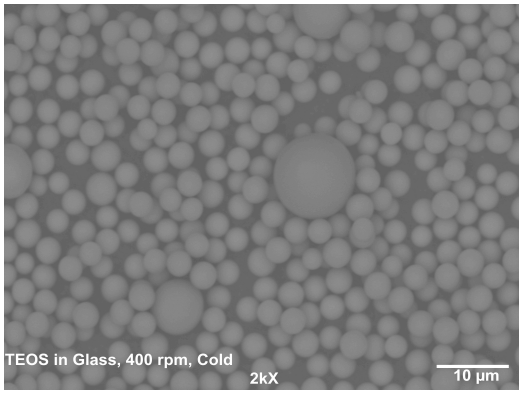

The micrograph in Image 21 demonstrates the relatively polydisperse nature of sample Q.

Image 22: Electron Micrograph of Sample R

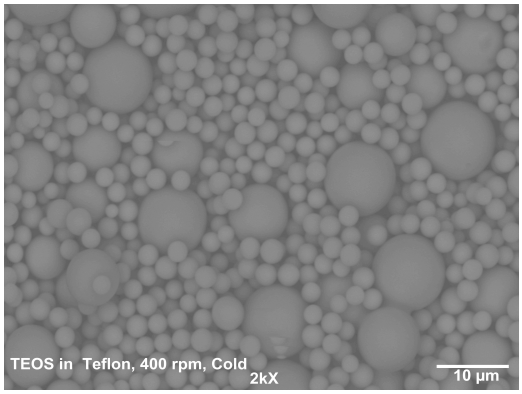

The micrograph in Image 22 demonstrates the relatively polydisperse nature of sample R. In addition, the micrograph displays aggregation of particles and particles with irregular surface morphologies.

Image 23: Electron Micrograph of Sample S

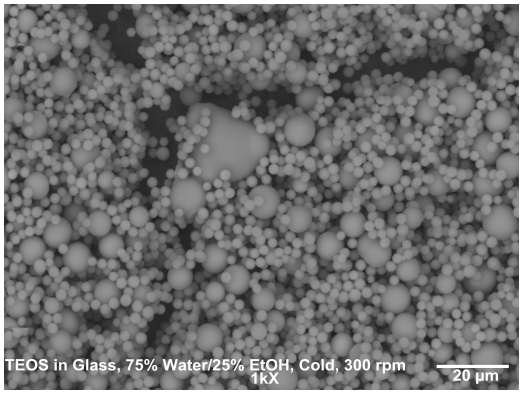

The micrograph in Image 23 demonstrates the relatively polydisperse nature of sample S. In addition, the micrograph displays aggregation of particles and particles with irregular surface morphologies.

Image 24: Electron Micrograph of Sample T

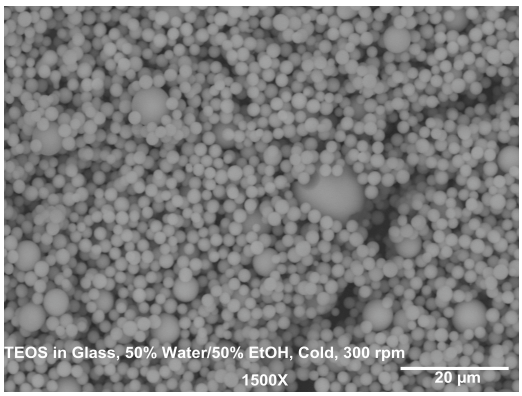

The micrograph in Image 24 demonstrates the relatively polydisperse nature of sample T.

Electron micrographs for Ag[Eu(EDTA)], K[Eu(acac)$_4$], and 5,10,15,20-Tetra(4-Pyridyl)-21H,23H porphine are presented in Images 25, 26, and 27, respectively. Luminescence data for Ag[Eu(EDTA)] and K[Eu(acac)$_4$] is presented in Figures 1 and 2, respectively. In addition, luminescence data for 5,10,15-20-Tetra(4-Pyridyl)-21H,23H porphine is presented in Figure 3.

Image 25: Electron Micrograph of Ag[Eu(EDTA)]

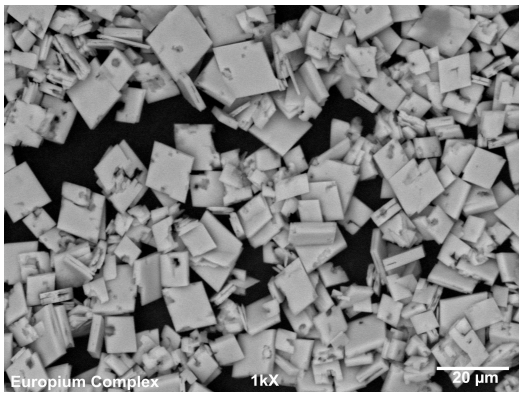

Figure 1: Luminescence of Ag[Eu(EDTA)] (λ_{EX} = 390 nm)

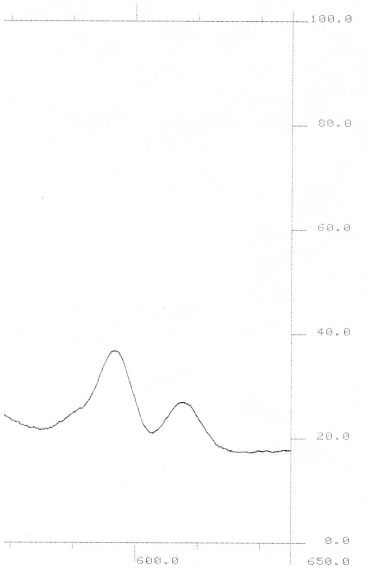

Figure 1 shows emission peaks at approximately 590 nm and 620 nm.

Image 26: Electron Micrograph of K[Eu(acac)$_4$]

Figure 2: Luminescence of $K[Eu(acac)_4]$ (λ_{EX} = 390 nm)

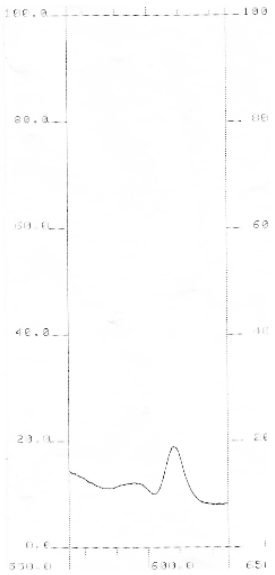

Figure 2 shows an emission peak at approximately 620 nm.

Image 27: Electron Micrograph of 5,10,15,20-Tetra(4-Pyridyl)-21H,23H porphine

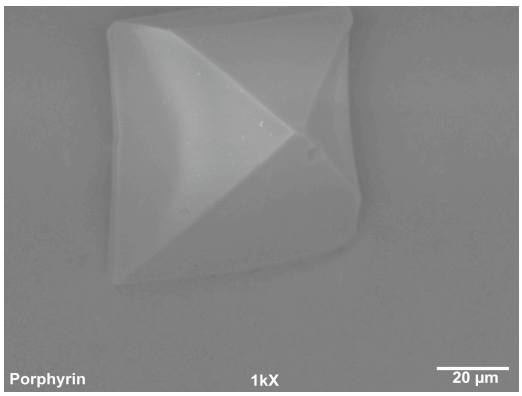

Figure 3: Luminescence of 5,10,15,20-Tetra(4-Pyridyl)-21H,23H porphine

(λ_{EX} = 500 nm)

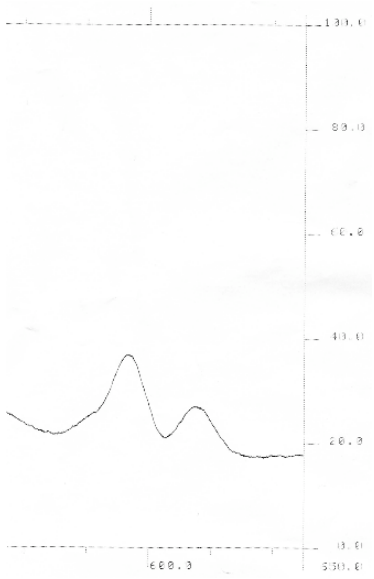

Figure 3 shows emission peaks at approximately 590 nm and 615 nm

Electron micrographs of silicates doped with coordination compounds of europium(III) are presented in Images 28, 29, and 32. Energy dispersive X-ray analysis (EDX) data for the silicates doped with coordination compounds of europium(III) are presented in Figures 4, and 5. Luminescence data for the silicates doped with coordination compounds of europium(III) are presented in Figures 6 and 8. Electron micrographs of silicates doped with 5,10,15,20-Tetra(4-Pyridyl)-21H,23H porphine are presented in Images 34 and 35. Luminescence data for the silicates doped with 5,10,15,20-Tetra(4-Pyridyl)-21H,23H porphine is presented in Figure 10. A low-magnification electron micrograph of a sample of silica microspheres is presented in Image 29 for comparison

with samples doped with europium(III) coordination compounds or 5,10,15,20-Tetra(4-Pyridyl)-21H,23H porphine. Luminescence data for the silica microspheres with excitation wavelengths relevant to the europium(III) coordination compounds and 5,10,15,20-Tetra(4-Pyridyl)-21H,23H porphine is presented in Figures 7, 9, and 11.

Image 28: Electron Micrograph of Microspheres Doped with Ag[Eu(EDTA)]

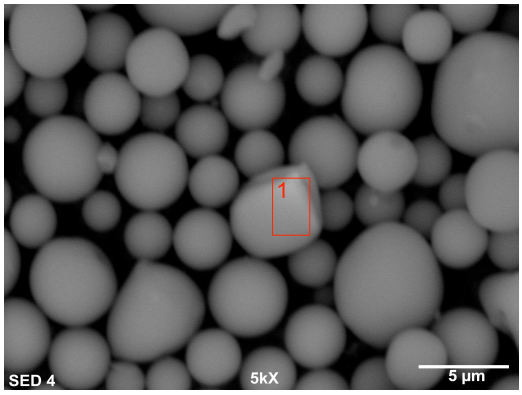

Figure 4: EDX Analysis of Selected Region In Image 28

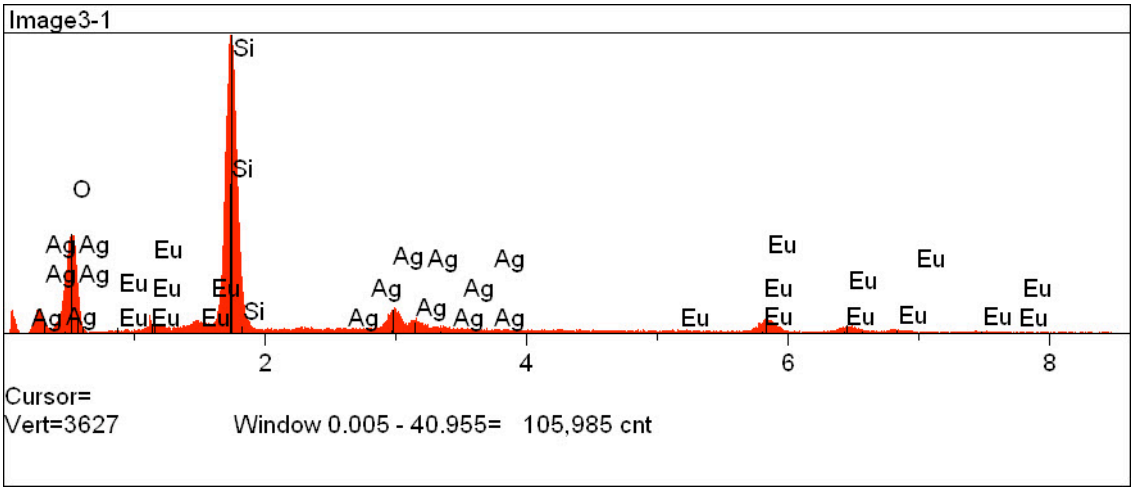

Image 28 displays a microsphere containing Ag[Eu(EDTA)]. The selected region in Image 28 was analyzed using EDX. The resulting spectrum, displayed in Figure 4, demonstrates the microsphere does contain the coordination compound.

Image 29: Electron Micrograph of Microspheres Doped with Ag[Eu(EDTA)]

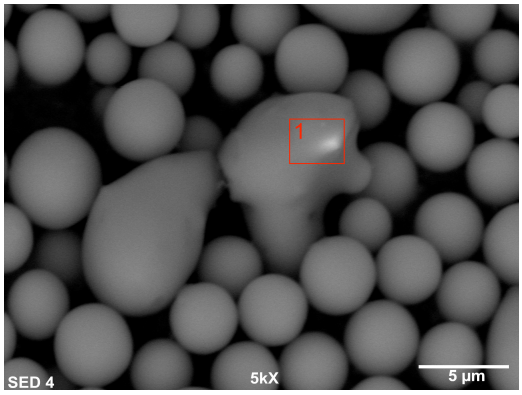

Figure 5: EDX Analysis of Selected Region In Image 29

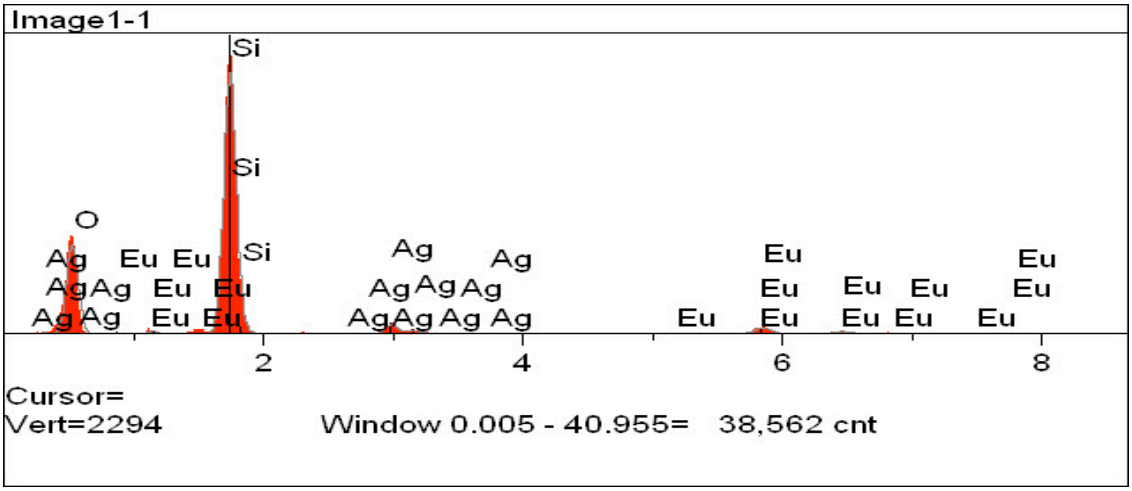

Image 29 displays a microsphere containing Ag[Eu(EDTA)]. The selected region in Image 29 was analyzed using EDX. The resulting spectrum, displayed in Figure 5, demonstrates the microsphere does contain the coordination compound.

Image 30: Low-Magnification Electron Micrograph of Microspheres Doped with Ag[Eu(EDTA)] Showing No Free Complex

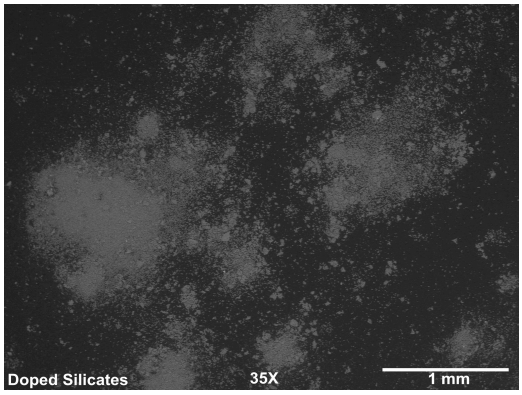

Image 31: Low-Magnification Electron Micrograph of Silica Microspheres

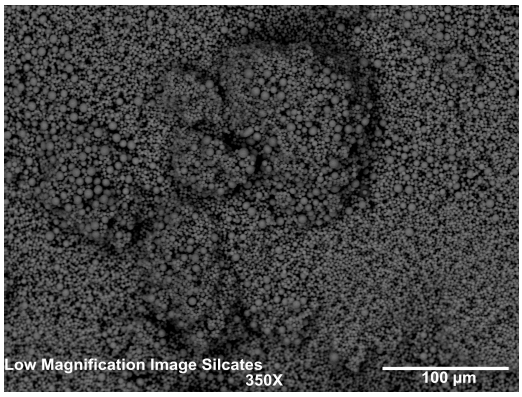

Comparison of Images 30 and 31 reveal the microspheres doped with Ag[Eu(EDTA)] (in Image 30) visibly resemble silica microspheres that do not contain the coordination

compound. Due to the high atomic mass of europium, the micrograph in Image 30 would display several bright areas surrounding the microspheres if free Ag[Eu(EDTA)] was present in the sample.

Figure 6: Luminescence of Sample in Image 30 (λ_{EX} = 390 nm)

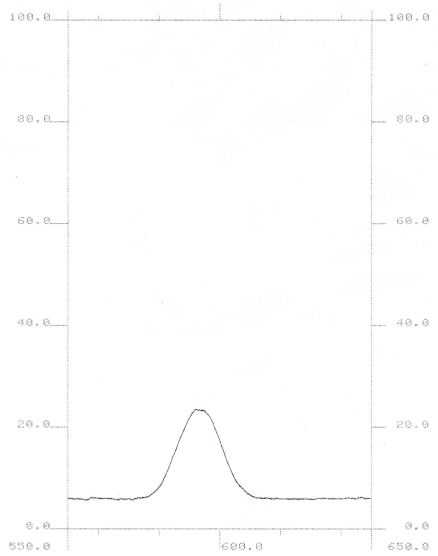

Figure 7: Luminescence of Sample in Image 31 (λ_{EX} = 390 nm)

Figure 6 represents the luminescence of the sample displayed in Image 30. The emission spectrum is consistent with that of Ag[Eu(EDTA)] presented in Figure 1. The emission peak at approximately 620 nm in Figure 1, known as the hypersensitive transition, is sensitive to the environment of the coordinated metal.[37] The absence of this peak in Figure 6 suggests interaction of the silica microsphere with the coordination sphere of the metal ion. Figure 7 demonstrates that silica microspheres do not luminesce in the region from 550 nm to 650 nm when excited with 390 nm light.

Image 32: Electron Micrograph of Microspheres Doped with $K[Eu(acac)_4]$

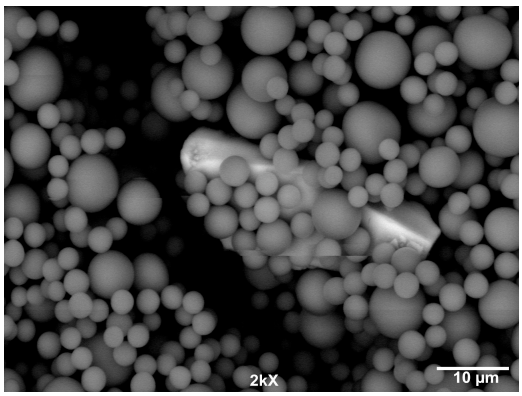

The electron micrograph in Image 32 presents a microcrystal of $K[Eu(acac)_4]$ that is coated with a silicate shell.

Image 33: Low-Magnification Electron Micrograph of Micro Silicates Doped with $K[Eu(acac)_4]$ Showing No Free Complex

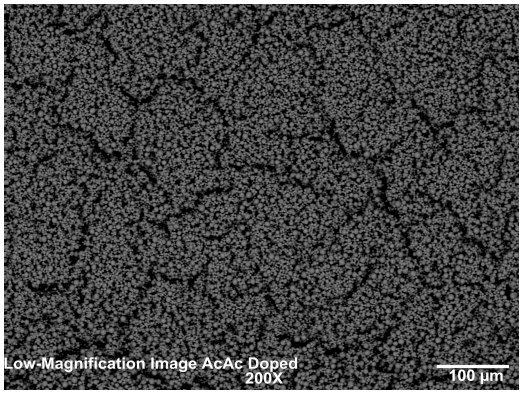

Comparison of Images 33 and 31 reveal the microspheres doped with $K[Eu(acac)_4]$ (in Image 33) visibly resemble silica microspheres that do not contain the coordination compound. Due to the high atomic mass of europium, the micrograph in Image 33 would display several bright areas surrounding the microspheres if free $K[Eu(acac)_4]$ was present in the sample.

Figure 8: Luminescence of Sample in Image 33 (λ_{EX} = 390 nm)

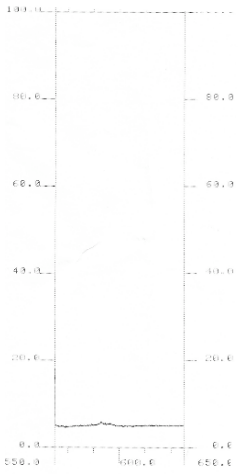

Figure 9: Luminescence of Sample in Image 31 (λ_{EX} = 390 nm)

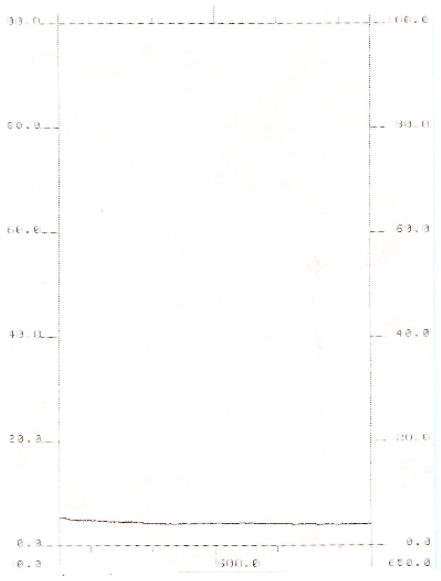

Figure 8 represents the luminescence of the sample displayed in Image 33. The emission spectrum of K[Eu(acac)$_4$] is presented in Figure 2. The absence of the hypersensitive transition peak at approximately 620 nm in Figure 8 could suggests interaction of the silica microsphere with the coordination sphere of the metal ion or attenuation of complex luminescence by the matrix. This could potentially lead to the lack of luminescence observed in Figure 8. Figure 9 demonstrates that silica microspheres do not luminesce in the region from 550 nm to 650 nm when excited with 390 nm light.

Image 34: Electron Micrograph of Microspheres Doped with 5,10,15,20-Tetra(4-Pyridyl)-21H,23H porphine

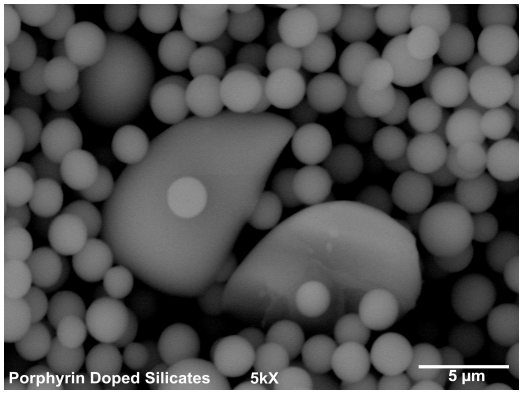

The electron micrograph in Image 34 presents silica microspheres with unusual structural features. The well-defined edge present in these microspheres suggests they may contain porphyrin crystals. Due to the low atomic mass of the elements composing the porphyrin macrocyle, the presence of a porphyrin within these microspheres is difficult to confirm through EDX analysis.

Image 35: Low-Magnification Electron Micrograph of Microspheres Doped with 5,10,15,20-Tetra(4-Pyridyl)-21H,23H porphine

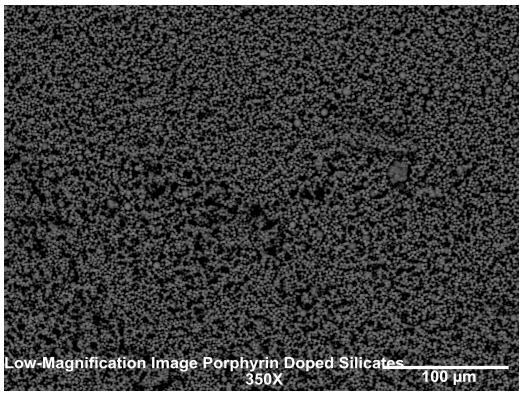

Comparison of Images 35 and 31 reveal the microspheres doped with 5,10,15,20-Tetra(4-Pyridyl)-21H,23H porphine (in Image 35) visibly resemble silica microspheres that do not contain the coordination compound. There are some microspheres in Image 35 that exhibit unusual structural features, and no free porphyrin crystals are observed.

Figure 10: Luminescence of Sample in Image 35 (λ_{EX} = 500 nm)

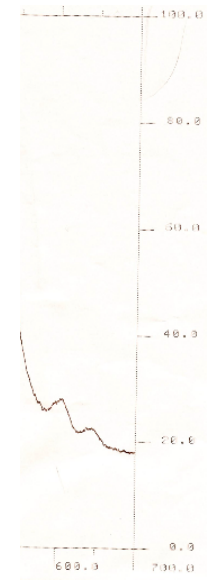

Figure 11: Luminescence of Sample in Image 31 (λ_{EX} = 500 nm)

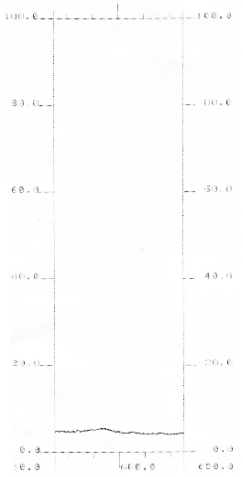

Figure 10 represents the luminescence of the sample displayed in Image 34. The emission spectrum is consistent with that of 5,10,15,20-Tetra(4-Pyridyl)-21H,23H porphine presented in Figure 3. The observed luminescence and absence of free porphyrin crystals suggests the porphyrin may be incorporated into the silica microspheres presented in Image 34. Figure 7 demonstrates that silica microspheres do not luminesce in the region from 550 nm to 650 nm when excited with 500 nm light.

CHAPTER 4

CONCLUSIONS

The unique optical properties of silica microspheres and lanthanoid elements present the opportunity to adapt silicates and lanthanoid coordination complexes for novel optical applications. The work has developed a reliable synthetic preparation of silica microspheres from the acid-catalyzed hydrolysis of TEOS. Reduction of the reaction temperature and the addition of ethyl alcohol to the mother liquor appeared to significantly retard the growth of the micro silicates and prevent undesirable particle aggregation. In addition, the rate of mixing during the hydrolysis reaction appeared to have an appreciable impact on particle uniformity. Lower reaction temperatures offer kinetic control over the hydrolysis reaction, while the presence of ethyl alcohol shifts the reaction equilibrium such that hydrolysis is less favored as predicted by Le Chatelier's Principle.

The research has also demonstrated the feasibility of incorporating crystalline europium(III) coordination complexes into micro silicates. Incorporation of Ag[Eu(EDTA)] has been confirmed via SEM, and the environment of the coordinated europium(III) ion has been probed using spectrofluorophotometry**.** This represents the first example of incorporating an insoluble lanthanoid ion complex into a silica microsphere. Luminescence data indicates the optical properties of the coordinated metal

center are retained upon incorporation into a silica microsphere. In addition, the data suggests the microsphere may interact with the coordination sphere of the metal center. The hyersenstive $5D_0 \rightarrow 7F_2$ transition, which results in an emission around 620 nm, is not observed for the coordination compounds that have been doped into silica microspheres. This could indicate the microsphere is directly interacting with the coordination environment of the metal. This lends credence to the proposal that incorporation of insoluble lanthanoid coordination compounds into silica microspheres could protect the metal center from ligands capable of quenching the metal luminescence. In order to confirm this suspicion, however, luminescence lifetime measurements of the doped and free coordination compounds must be obtained. If the silica microsphere does in fact protect the metal complex from the chemical environment, then these novel structures could have numerous optical applications. The potential application of doped silica microspheres in biologically relevant studies has generated recent interest. Specifically, silica microspheres containing luminescent lanthanoid ions and having surfaces functionalized with organic linker groups have been used as fluorescent tags for immunoassay studies.[37] The potential biocompatibility of doped micro silicates, then, poses the opportunity to adapt silicates containing lanthanoid coordination complexes as wavelength specific sensors for protein studies or immunoassay detectors. The doped microspheres would also be amenable to many additional optical applications for which silica microspheres or sol-gels containing lanthanoid ions have been used (*vide supra*).

Incorporation of $K[Eu(acac)_4]$ into a silica shell has also been confirmed via SEM. Luminescence of the doped complex, however, was not observed. The luminescence of the free complex (see Figure 2) shows primary emission at approximately 620 nm, and

virtually no emission at approximately 590 nm. The lack of luminescence for the doped microsilicates could possibly indicate quenching of emission from the hypersensitive transition by a silicate coating around the complex. The lack of luminescence could also indicate attenuation of the complex luminescence by the silica matrix. Silver(I) ions have been shown to enhance the luminescence of europium(III) salts, and this could account for the fact that luminescence is observed for Ag[Eu(EDTA)] when the complex is doped into silica microspheres.[31] That is, the enhancement from the silver(I) counter-ion could potentially be more substantial than the attenuating effects of the silica matrix. $K[Eu(acac)_4]$, however, does not experience emission enhancement from a silver(I) counter-ion, and the matrix attenuation could potentially reduce the intensity of the complex emission to such a degree that the emission is no longer detectable. The lack of luminescence for the doped silicates, then, could support the conclusion that silicate coatings around a europium(III) coordination compound could potentially interact with the coordination sphere of the metal center or attenuate the luminescence of incorporated lanthanoid complexes.

AFM characterization of the surface morphology of the micro silicates did not provide significant insight into potential surface interactions that could influence particle formation. The surface structures of the micro silicates were found to be sufficiently small (i.e. nanometer scale) to prevent the work from drawing any significant conclusions. The research anticipated the presence of larger, non-uniform surface features that would indicate potential surface interactions between particles or between the particles and the reaction vessel. However, the relatively uniform and smooth surface of the particles presented no indication of these interactions.

Complexes of europium(III) with highly conjugated ring systems, such as porphyrins, are particularly interesting because the macrocycle has the potential to serve as an antenna that harvests photons. Unfortunately, the synthesis of such complexes often involves reagents or solvents that are detrimental to the environment. The research envisioned synthetic preparations that are more environmentally compatible, and the research attempted to develop an entirely aqueous synthesis. The initial approach involved protonating the pyridyl moieties of 5,10,15,20-Tetra(4-Pyridyl)-21H,23,H porphine to generate a charged, water soluble porphyrin system. A variety of reaction temperatures and times, as well as a variety of europium(III) sources, were explored. These preliminary attempts to synthesize monoporphyrinate europium(III) complexes were unsuccessful, however. The desired monoporphyrinate was not isolated under the experimental conditions, and UV-Visable spectroscopy revealed the only isolated product was the porphyrin reagent. The research then attempted several syntheses utilizing 1-Pentanol as the solvent, but the target monoporphyrinate was not isolated under the experimental conditions. Due to time constraints, the research attempted a traditional synthesis of the monoporphyrinate using 1,2,4-Trichlorobenzene as the solvent in order to explore the viability of incorporating these macrocyclic complexes into silica microspheres. Unfortunately, the desired monoporphyrinate was not isolated. In an attempt to demonstrate the feasibility of doping europium(III) monoporphyrinates into silica microspheres, the research explored the incorporation of 5,10,15,20-Tetra(4-Pyridyl)-21H,23,H porphine into microspheres. Due to the low atomic mass of the elements composing the macrocycle, SEM does not provide evidence that significantly suggests the presence of the porphyrin within the microspheres. However, the unusual

structural features and coloration of the doped silicates suggest the microspheres may contain porphyrin rings. This conclusion is supported by the fact that the luminescence of the doped microspheres is consistent with the luminescence observed for 5,10,15,20-Tetra(4-Pyridyl)-21H,23H porphine, despite the fact that no free porphyrin within the doped sample was observed using SEM. While further investigation is required, these preliminary results may suggest the feasibility of incorporating lanthanoid monoporphyrinates into silica microspheres.

Future research will continue to explore the synthesis of europium(III) monoporphyrinate complexes and the necessary reaction parameters for incorporating these complexes into silica microspheres. The research will attempt to optimize the synthesis of monodisperse micro silicates that contain europium(III) complexes. In addition, the interaction of the silica microsphere with the coordination environment of incorporated europium(III) complexes will be explored through luminescence lifetime measurements. The research will attempt to synthesize a novel tetrakis(2,4-pentanediono)europate(III) complex containing a silver(I) counter-ion to explore the attenuating effects of the silica matrix.

REFERENCES

1. Gao, X.; Nie, S. Quantum-Dot Encoded Mesoporous Beads with High Brightness and Uniformity: Rapid Readout Using Flow Cytometry. *Anal. Chem.* **2004**, *76*, 2406-2410.
2. Ho, Y.; Kung, M.; Yang, S.; Wang, T. Multiplexed Hybridization Detection with Multicolor Colocalization of Quantum Dot Nanoprobes. *Nano Letters*. **2004**, *5*, 1963-1967.
3. Sathe, T.; Agrawal, A.; Nie, S. Mesoporous Silica Beads Embedded with Semiconductor Quantum Dots and Iron Oxide Nanocrystals: Dual-Function Microcarriers for Optical Encoding and Magnetic Separation. *Anal. Chem.* **2006**, *78*, 5627-5632.
4. Battersby, B.; Bryant, D.; Meutermans, W.; Matthews, D.; Smythe, M.; Trau, M. Toward Larger Chemical Libraries: Encoding with Fluorescent Colloids in Combinatorial Chemistry. *J. Am. Chem. Soc.* **2000**, *122*, 2138-2139.
5. Gao, X.; Nie, S. Doping Mesoporous Materials with Multicolor Quantum Dots. *J. Phys. Chem. B*. **2003**, *107*, 11575-11578.
6. Yi, D.; Selvan, S.; Lee, S.; Papaefthymiou, G.; Kundaliya, D.; Ying, J. Silica-Coated Nanocomposites of Magnetic Nanoparticles and Quantum Dots. *J. Am. Chem. Soc.* **2005**, *127*, 4990-4991.

7. Gerion, D.; Parak, W.; Williams, S.; Zanchet, D.; Micheel, C.; Alivisatos, A. Sorting Fluorescent Nanocrystals with DNA. *J. Am. Chem. Soc.* **2002**, *124*, 7070-7074.

8. Ma, D.; Guan, J.; Normandin, F.; Denommee, S.; Enright, G.; Veres, T.; Simard, B. Multifunctional Nano-Architecture for Biomedical Applications. *Chem. Mater.* **2006**, *18*, 1920-1927.

9. Mulder, W.; Koole, R.; Brandwijk, R.; Storm, G.; Chin, P.; Strijkers, G.; Donega, C.; Nicolay, K.; Griffioen, A. Quantum Dots with a Paramagnetic Coating as a Bimodal Molecular Imaging Probe. *Nano Letters*. **2006**, *6*, 1-6.

10. Wang, D.; He, J.; Rosenzweig, N.; Rosenzweig, Z. Superparamagnetic Fe_2O_3 Beads – CdSe/ZnS Quantum Dots Core – Shell Nanocomposite Particles for Cell Separation. *Nano Letters*. **2004**, *4*, 409-413.

11. Guo, J.; Yang, W.; Wang, C.; He, J.; Chen, J. Poly(N-isopropylacrylamide)-Coated Luminescent/Magnetic Silica Microspheres: Preparation, Characterization, and Biomedical Applications. *Chem Mater.* **2006**, *18*, 5554-5562.

12. Dubreuil, N.; Knight, J.; Leventhal, D.; Sandoghdar, V.; Hare, S.; Lefevre, V. Eroded monomode optical fiber for whispering-gallery mode excitation in fused-silica microspheres. *Optics Letters*. **1995**, *20*, 813-815.

13. Cai, M.; Painter, O.; Vahala, K. Observation of Critical Coupling in a Fiber Taper to a Silica-Microsphere Whispering-Gallery Mode System. *Phys. Rev. Letters*. **2000**, *85*, 74-77.

14. Spillane, S.; Kippenberg, T.; Painter, O.; Vahala, K. Ideality in a Fiber-Taper-Coupled Microresonator System for Application to Cavity Quantum Electrodynamics. *Phys. Rev. Letters*. **2003**, *91*, 1-4.

15. Suzuki, H.; Tombrello, T.; Melcher, C.; Schweitzer, J. UV and gamma-ray excited luminescence of cerium-doped rare-earth oxyorthosilicates. *Nuclear Instruments and Methods in Physics Research*. **1992**, 263-272.

16. Sololnicki, J. Photoluminescence and structural characteristics of $Lu_2O_3:Eu^{3+}$ nanocrystallites in silica matrix. *J. Solid State Chem.* **2007**, *180*, 2400-2408.

17. Iwanczyk, J.; Patt, B.; Tull, C.; Macdonald, L; Bescher, E.; Robson, S.; Mackenzie, J.; Hoffman, E. New LSO Based Scintillators. *IEEE Transactions On Nuclear Science*. **2000**, *47*, 1781-1786.

18. Koester, C.; Snitzer, E. Amplification in a fiber laser. *Appl. Optics*. **1964**, *3*, 1182-1186.

19. Miyajima, Y.; Komukai, T.; Sugawa, T. 1.31-1.36 μm optical amplification in Nd^{3+}-doped Fluorozirconate Fibre. *Electron. Lett.* ***1990,*** *26*, 194-195.

20. Chen, C.; Choy, M.; Andrejco, M.; Saifi, M.; Lin, C. A widely tunable erbium-doped fiber laser pumped at 532 nm. *IEEE Photon. Technol. Lett.* **1990**, *2*, 18-20.

21. Davey, R.; Langford, N.; Ferguson, A. Subpicosecond pulse generation from erbium doped fiber laser. *Electron. Lett.* **1991**, *27*, 726-728.

22. Enrichi, F. Luminescent Amino-functionalized or Erbium-doped Silica Spheres for Biological Applications. *Annal. New York Acad. Sci.* **2008**, *1130*, 262-266.

23. Bunzil, J.; Piguet, C. Taking advantage of luminescent lanthanide ions. *Chem. Soc. Rev.* **2005**, *34*, 1048-1077.

24. Soares-Santos, P.; Nogueira, H.; Felix, V.; Drew, M.; Sa Ferreira, R.; Carlos, L.; Trindade, T. Novel Lanthanide Luminescent Materials Based on Complexes of 3-Hyroxypicolinic Acid and Silica Nanoparticles. *Chem. Mater.* **2003**. *15*, 100-108.

25. Arnaud, N.; Georges, J. Comprehensive Study of the Luminescent Properties and Lifetimes of Eu^{3+} and Tb^{3+} Chelated with Various Ligands in Aqueous Solutions: Influence of the Synergic Agent, the Surfactant, and the Energy Level of the Ligand Triplet. *Spectrochem. Acta A*. **2003**, *59*, 1829-1840.

26. Latva, M.; Takalo, H.; Mulkala, V.; Matachescu, C.; Rodriguez-Ubis, J.; Kankare, J. Correlation Between the Lowest Triplet State Energy Level of the Ligand and Lanthanide(III) Luminescence Quantum Yield. *J. Lumin.* **1997**, *75*, 149-169.

27. Li, X.; Qiu, J.; Zhang, L.; Mu, J. In-situ Synthesis and Photoluminescence of a Europium Porphyrin Complex Incorporated in the Silica Matrix. *J. Dispers. Sci. Technol.* **2007**, *28*, 1081-1085.

28. Rossi, L.; Shi, L.; Quina, F.; Rosenzweig, Z. Stober Synthesis of Monodisperesed Luminescent Silica Nanoparticles for Bioanalytical Assays. *Langmuir*. **2005**, *21*, 4277-4280.

29. de Dood, M.; Berkhout, B.; can Kats, C.; Polman, A.; Blaaderen, A. Acid-Based Synthesis of Monodisperse Rare-Earth-Doped Colloidal SiO_2 Spheres. *Chem. Mater.* **2002**, *14*, 2849-2853.

30. Gorodetsky, M.; Pryamikov, A. Rayleight scattering in high-Q microspheres. *J. Opt. Soc. Am. B*. **2000**, *17*, 1051-1057.

31. Pesterfield, L. High-Resolution Luminescence Spectroscopy of Selected Eu(III) Ion Complex Salts. University of Tennessee, Knoxville. **1991**.

32. Murray, G. Rare Earth Containing Complex Compounds for the Determination of Inorganic Ions. University of Tennessee, Knoxville. **1988**.

33. Spyroulias, G.; Raptopoulou, C.; de Montauzon, D.; Mari, A.; Poilblanc, R.; Terzis, A.; Coutsolelos, A. Synthesis and Physiochemical Characterization of Protonated and Deprotonated Forms in Heteroleptic Lanthanide(III) Porphyrinate Double-Deckers. X-ray Structure of $Gd^{III}H(ope)(tpp)$ at 298 and 21 K. *Inorg. Chem.* **1999**, *38*, 1683-1696.

34. Spyroulias, G.; Coutsolelos, A.; Raptopoulou, C.; Terzis, A. Synthesis, Characterization, and X-ray Study of a Heteroleptic Samarium(III) Porphyrin Double-Decker Complex. *Inorg. Chem.* **1995**, *34*, 2476-2479.

35. Wong, C.; Venteicher, R.; Horrocks, W. Lanthanide Porphyrin Complexes: A Potential New Form of Nuclear Magnetic Resonance Dipolar Probe. *J. Am. Chem. Soc.* **1974**, *96*, 7149-7150.

36. Binnemans, K.; Van Herck, K.; Gorller-Walrand, C. Influence of dipicolinate ligands on the spectroscopic properties of europium(III) in solution. *Chem. Phys. Lett.* **1997**, *266*, 297-302.

37. Ye, Z.; Tan, M.; Wang, G.; Yuan, J. Preparation, Characterization, and Time-Resolved Fluorometric Applications of Silica-Coated Terbium(III) Fluorescent Nanoparticles. *Anal. Chem.* **2004**, *76*, 513-518.